A second order time-stepping scheme for parabolic interface problems with moving interfaces

Stefan Frei* Thomas Richter †

Preprint, June 2016

Abstract

We present a second order time-stepping scheme for parabolic problems on moving domains and interfaces. The diffusion coefficient is discontinuous and jumps across an interior interface. This causes the solution to have discontinuous derivatives in space and time. Without special treatment of the interface, both spatial and temporal discretization will be sub-optimal.

For such problems, we develop a time-stepping method, based on a cG(1) Eulerian space-time Galerkin approach. We show - both analytically and numerically - second order convergence in time. Key to gaining the optimal order of convergence is the use of space-time test- and trial-functions, that are aligned with the moving interface.

Possible applications are multiphase flow or fluid-structure interaction problems.

1 Introduction

Interface problems, where the solution has discontinuities or discontinuous derivatives along an interface through the domain appear as typical part of various applications. Viscous multiphase-problems, where two fluids with different physical parameters (like viscosity or density) are coupled at a common interface, have a continuous velocity on the complete domain. Across the interface, however, the velocity is not differentiable, neither in space nor in time. Fluid-structure interactions show a similar behaviour: the kinematic coupling condition calls for a continuous transition of the fluid to the solid velocity, this coupling, however, is not differentiable. A simple example for such an interface problem is the following parabolic model problem. Let

$$Q := \{(t,\Omega(t)),\ t \in I := [0,T]\} \subset \mathbb{R}^{d+1},$$

be a convex space-time domain, that is split into two sub-domains $Q = Q_1 \cup G \cup Q_2$ by an interface $G \subset \mathbb{R}^d$, where $\Omega(t) = \Omega_1(t) \cup \Gamma(t) \cup \Omega_2(t)$:

$$Q_i := \{(t,\Omega_i(t)),\ t \in I := [0,T]\} \subset \mathbb{R}^{d+1}, \quad G := \{(t,\Gamma(t)),\ t \in I := [0,T]\}.$$

(cf. Figure 1). Given $u^0 \in L^2(\Omega(0))$, we define the model problem by

$$\begin{aligned} \partial_t u_i - \operatorname{div}\left(\kappa_i \nabla u_i\right) &= f_i && \text{in } Q_i,\ i=1,2, \\ u_1 = u_2, \quad \mathbf{n}\cdot\kappa_1\nabla u_1 &= \mathbf{n}\cdot\kappa_2\nabla u_2 && \text{on } \Gamma(t), \\ u(\cdot,0) &= u^0 && \text{on } \Omega(0), \\ u(\cdot,t) &= 0 && \text{on } \partial\Omega(t), \end{aligned} \tag{1}$$

*Institute of Applied Mathematics, Heidelberg University, Im Neuenheimer Feld 205, 69120 Heidelberg, Germany (stefan.frei@iwr.uni-heidelberg.de)

†Friedrich-Alexander-University Erlangen-Nuremberg, Department Mathematics AM3, Cauerstraße 11, 91058 Erlangen (richter@math.fau.de)

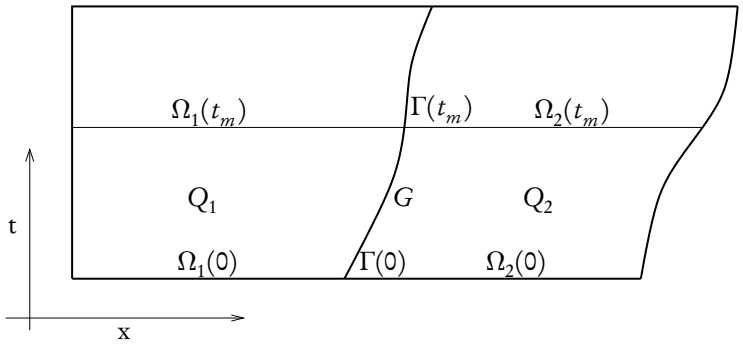

Figure 1. Space-time domain. Both the interface $\Gamma(t)$ and the outer boundary $\partial\Omega(t)$ might move in time.

where the diffusion coefficient $\kappa : Q \to \mathbb{R}$ takes two values $\kappa_1, \kappa_2 \in \mathbb{R}$ in the sub-domains Q_1, Q_2. On smooth domains $Q = Q_1 \cup G \cup Q_2$, given sufficient regularity of the right hand side f, an initial data u^0 that satisfies the compatibility conditions $-\kappa\Delta u^0 - f \in H_0^1(\Omega(0))$ and $\kappa_1 \mathbf{n} \cdot \nabla u_1^0 = \kappa_2 \mathbf{n} \cdot \nabla u_2^0$ and positive diffusion coefficients $\kappa_1, \kappa_2 > 0$, this problem has a solution $u = \{u_1, u_2\}$ that satisfies [9]

$$\sum_{k=0}^{2} \|u\|_{k,2(2-k)} \leq c \left(\sum_{k=0}^{1} \|f\|_{k,2(1-k)} + \|u^0\|_{H^4(\Omega_1(0)\cup\Omega_2(0))} \right). \tag{2}$$

If we have additionally the compatibility condition $\partial_t f(0) - \kappa_i \Delta f(0) + \kappa_i^2 \Delta^2 u^0 \in H_0^1(\Omega_i(0))$ and sufficient regularity of the data f, u^0, it holds that

$$\sum_{k=0}^{3} \|u\|_{k,2(3-k)} \leq c \left(\sum_{k=0}^{2} \|f\|_{k,2(2-k)} + \|u^0\|_{H^6(\Omega_1(0)\cup\Omega_2(0))} \right). \tag{3}$$

Here, we have used the norms

$$\|u\|_{k,l} := \left(\|u\|^2_{H^k(I,H^l(\Omega_1(t)))} + \|u\|^2_{H^k(I,H^l(\Omega_2(t)))} \right)^{1/2}$$

on the Bochner spaces

$$\mathscr{H}^{k,l} := H^k(I, H^l(\Omega_1(t))) \cap H^k(I, H^l(\Omega_2(t)))$$

that are based on the usual Sobolev spaces H^k, H^l in space and time. By $H^0(\Omega)$ we denote the Lebesgue space $L^2(\Omega)$. The solution u has no higher global spatial or temporal regularity across the interface $G := \{(t, \Gamma(t)),\ t \in I\}$, instead it carries a *weak discontinuity* in space and time.

Considering the discretization of such interface problems, we have to deal with two difficulties. *First, the spatial discretization* is known to fail for interface-problems [2], if the finite element mesh does not resolve the interface, i.e., at time $t = t_m$, there must be a compatible finite element space, that is able to resolve the interface in such a way, that accurate interpolation results hold

$$\|u - i_h u\|_\Omega + h\|\nabla(u - i_h u)\|_\Omega \leq c h^{r+1} \left(\|\nabla^{r+1} u\|_{\Omega_1} + \|\nabla^{r+1} u\|_{\Omega_2} \right).$$

This is either achieved by using fitted finite element meshes (see e.g. [5]) with triangulations of the two sub-domains, or by enrichment of standard spaces on non-fitted meshes with additional basis functions. A prominent example for such a technique is the extended finite element method

(XFEM), see [16]. An alternative, very simple approach, that is based on a local parametric finite element space on standard unfitted meshes has been presented by the authors [12].

Second, and this is the topic of the paper at hand, the temporal discretization is a major challenge. The method of lines cannot be applied, if the domain $\Omega(t) \subset \mathbb{R}^d$ is changing in time. Rothe's method relies on time-stepping $t_{m-1} \to t_m$. In the usual finite element setting, applying a simple one-step method like the backward Euler scheme, Rothe's method for the parabolic model problem reads:

$$\frac{1}{t_m - t_{m-1}}(u^m - u^{m-1}, \phi) + (\kappa \nabla u^m, \nabla \phi) = (f(t_m), \phi) \quad \forall \phi \in V(t_m), \tag{4}$$

where $u^{m-1} \in V(t_{m-1})$ is the solution at time t_{m-1} and $u_m \in V(t_m)$ is the sought solution at time t_m. But again, in the case of moving domains, it holds $\Omega(t_{m-1}) \neq \Omega(t_m)$ and therefore $V(t_{m-1}) \neq V(t_m)$. The problem comes to the fore, if one considers the role of the scalar product $(u^m - u^{m-1}, \phi) = \int_\Omega (u^m - u^{m-1})\phi \, \mathrm{d}x$. Whether we choose $\Omega(t_{m-1})$ or $\Omega(t_m)$ as domain for integration, the integral is not defined for one of the solutions u^m or u^{m-1}.

Next, let us consider interface problems on a fixed domain $Q := I \times \Omega$ where only the interior interface moves, but where the outer boundary is fixed. Here, the problem looks less severe. Equation (4) is well defined. However, consider a point $x \in \Omega$ with $x \in \Omega_1(t_{m-1})$ and $x \in \Omega_2(t_m)$ close to the interface. Then, by $(u^m(x) - u^{m-1}(x))/(t_m - t_{m-1})$, no approximation to the time-derivative u' is given, as u is not differentiable across the interface.

In the context of the extended finite element method, recent advances have been made in literature for this problem. Fries and Zilian [13] presented a time-stepping scheme based on the backward Euler method and a number of numerical tests that indicate first-order convergence order. A complete error analysis for this approach has been presented by Zunino [19]. For a corresponding Crank-Nicolson-like approach, Fries and Zilian found a reduced convergence order of 1.5. To the best of our knowledge, there is, however, no rigorous convergence analysis available yet. A second-order scheme based on a space-time dG(1) approach has been presented by Lehrenfeld and Reusken [15] including error analysis in space and time. Their approach can not be generalized to a continuous Galerkin scheme, however, as the spatial number of unknowns varies from time step to time step in their scheme.

Another approach to construct accurate time-stepping schemes is to apply a transformation to a fixed reference domain $\hat{Q} := I \times \{\hat{\Omega}_1 \cup \hat{\Gamma} \cup \hat{\Omega}_2\}$. Let $\hat{T} : \hat{Q} \to Q$ be such a mapping. If $\hat{T}$ is a C^2-diffeomorphism, Problem (1) is equivalent to

$$\det(\hat{\nabla}\hat{T})\left(\partial_t \hat{u} - \partial_t \hat{T} \cdot \nabla \hat{u}\right) - \widehat{\mathrm{div}}\left(\det(\hat{\nabla}\hat{T})\hat{\kappa}\hat{\nabla}\hat{T}^{-1}\hat{\nabla}\hat{u}\hat{\nabla}\hat{T}^{-T}\right) = \det(\hat{\nabla}\hat{T})\hat{f} \text{ in } \hat{Q}. \tag{5}$$

This is the ALE-transform of the parabolic model problem (see e.g. [3]). Here, the domain $\hat{\Omega}$ allows a fixed partitioning $\hat{\Omega} = \hat{\Omega}_1 \cup \hat{\Gamma} \cup \hat{\Omega}_2$ that does not change in time. Standard spatial and temporal discretization is possible. However, the ALE approach only works, if a mapping $\hat{T} : \hat{Q} \to Q$ with sufficient regularity can be constructed.

In this paper, we follow a different approach: we start by designing a space-time Galerkin method on the space-time slots $Q^m = \{(t, \Omega(t)),\ t \in [t_{m-1}, t_m]\}$. In literature, this approach is known as the *continuous Galerkin (cG) method*, see [1,10], and a Galerkin scheme of Crank-Nicolson type is found by using continuous and piece-wise linear trial functions combined with discontinuous piece-wise constant test-functions. However, on space-time elements close to the (moving) interface or (moving) outer boundaries, we choose trial-functions, that are aligned to the element's faces: the solution is not linear in direction of time t, but linear in directions that stay within each subdomain or follow the interface line, see Figure 3.

The resulting time-stepping scheme can be seen as a moving-mesh approach where the reference domain changes in each time step. Thus, it may be considered a variant of the Fixed-mesh ALE

method proposed by Codina and co-workers in [6] in combination with a projection scheme that is based on projecting residuals. In the Fixed-mesh ALE method, the authors apply a moving mesh (ALE) technique in each time interval, but project the solution back to an original fixed mesh afterwards. In this way, the requirement of global regularity of an ALE map is reduced to local regularity within one time interval. As the relative movement of boundaries and interfaces with respect to the previous time step is typically rather small, the method is able to deal with large movements.

The novelty in this work are the application of a Galerkin time discretization within this framework rather than using a finite difference scheme and the usage of a residual-based projection. This enables us to derive a priori error estimates of optimal (second) order. To the knowledge of the authors no convergence results are available within the Fixed-mesh ALE framework yet in literature.

The outline of the paper is as follows: Section 2 details the space-time Galerkin approach and derives a corresponding time-stepping method. In Section 3, we derive a priori estimates for the temporal discretization error in the space-time L^2-norm and in the L^2-norm at the end time. In Section 4, we give some details on our practical implementation, with focus on numerical integration. Then, in Section 5, we will substantiate these results by numerical test-cases. We conclude in Section 6.

2 Time discretization

A variational formulation of (1) is given by: Find $u \in X$ such that

$$\begin{aligned} B(u,\phi) &= (f,\phi)_Q + (u^0, \phi(0))_{\Omega(0)} \quad \forall\, \phi \in X, \\ B(u,\phi) &:= (\partial_t u, \phi)_Q + (\kappa \nabla u, \nabla \phi)_Q + (u(0), \phi(0))_{\Omega(0)} \end{aligned} \tag{6}$$

where

$$(f,g)_Q := \int_0^T (f(t), g(t))_{\Omega(t)} \, \mathrm{d}s, \tag{7}$$

and

$$X := W(0,T) = \left\{ v : Q \to \mathbb{R} \;\middle|\; v \in L^2(I, H_0^1(\Omega(t))),\, \partial_t v \in L^2(I, H^{-1}(\Omega(t))) \right\}.$$

Due to the continuous embedding $W(0,T) \subset C(I, L^2(\Omega(t)))$, point values $u(t_i)$ in time are well-defined and hence the initial condition can be included into the variational formulation as in (6). The well-posedness of this variational problem for moving outer boundaries has been studied in [9].

In order to derive a time-stepping scheme, we split the time interval into discrete subintervals

$$I = \{0\} \cup I_1 \cup I_2 \cup \ldots \cup I_M, \quad I_j = (t_{j-1}, t_j].$$

For $j = 1, \ldots, M$, we denote the resulting space-time slabs by $Q^j := \{(x,t) \mid t \in I_j,\, x \in \Omega(t)\}$ and the space-time slabs corresponding to the subdomains by $Q_i^j := \{(x,t) \mid t \in I_j, x \in \Omega_i(t)\}$, $(i = 1,2)$. Let us for a moment assume that the outer boundary $\partial\Omega(t)$ is fixed such that $\Omega(t) = \Omega$ for all times t. Then, similar to (4), we can write down a simple time-stepping scheme of Crank-Nicolson type

$$\begin{aligned} \frac{1}{k}(u^m - u^{m-1}, \phi)_\Omega + \frac{1}{2}(\kappa(t_m)\nabla u^m, \nabla\phi)_\Omega + \frac{1}{2}(\kappa(t_{m-1})\nabla u^{m-1}, \nabla\phi)_\Omega \\ = \frac{1}{2}(f(t_m), \phi)_\Omega + \frac{1}{2}(f(t_{m-1}), \phi)_\Omega \quad \forall \phi \in H_0^1(\Omega). \end{aligned} \tag{8}$$

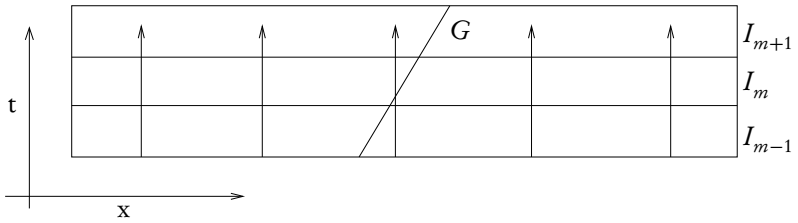

Figure 2. Space-time domain for a fixed outer domain $\Omega(t) = \Omega$. Functions $v_k \in \tilde{X}_k^0, \tilde{X}_k^1$ are polynomial on vertical lines (e.g. the indicated arrows).

Remember that in the case of a moving outer boundary, it is not straight-forward to write down a corresponding formulation, as u^m and u^{m-1} are defined on different domains $\Omega(t_m)$ and $\Omega(t_{m-1})$. It is well known that the Crank-Nicolson scheme (8) is equivalent to a space-time variational formulation with the following Galerkin trial and test spaces

$$\begin{aligned} u_k \in \tilde{X}_k^1 &= \left\{ v \in C(\bar{I}, H_0^1(\Omega)) \;\middle|\; v_{|I_m} \in P_1(I_m, H_0^1(\Omega)), v(0) \in H_0^1(\Omega) \right\} \\ \phi_k \in \tilde{X}_k^0 &= \left\{ v \in L^2(I, H_0^1(\Omega)) \;\middle|\; v_{|I_m} \in P_0(I_m, H_0^1(\Omega)), v(0) \in H_0^1(\Omega) \right\}. \end{aligned} \tag{9}$$

If the coefficient κ was continuous across the interface (in our case $\kappa_1 = \kappa_2$), second order convergence estimates for the discretization error would be straight-forward. This is not the case for a discontinuous coefficient, however, as the scheme does not account for the (moving) discontinuity of κ, f and ∇u at G. Instead the functions $u_k \in \tilde{X}_k^1$ are polynomial on space-time lines τ that cross the interface (e.g. the arrow crossing the interface in Figure 2), which means $u_k \in C^\infty(\tau)$. It follows that, in general, there is no second-order in time interpolant within the space $\tilde{X}_k^1$ and we can only expect a reduced order of convergence.

To derive a second-order scheme (that will also be usable for moving outer boundaries), we introduce a modified continuous Galerkin ansatz in time. Therefore, we define a Galerkin space of functions that are polynomial on trajectories that stay within the subdomains and are aligned to the space-time boundary and the interface in their vicinity. The construction of second-order interpolants in time will be straight-forward within this space. For deriving error estimates, it would be most convenient to introduce smooth global trajectories in the whole time-interval I. In practice, however, it is often a challenging task to define sufficiently smooth trajectories (consider for example large movements of the interface). Furthermore, the interface movement often depends on the solution itself and is therefore only known from time step to time step. Therefore, we define the trajectories piecewise in each time interval I_m (see Figure 2).

Specifically, we define the following (semidiscrete) test and trial spaces:

$$\begin{aligned} u_k \in X_k^1 &= \left\{ v \in C(\bar{I}, H_0^1(\Omega(t))) \;\middle|\; (v \circ T_m)_{|I_m} \in P_1(I_m, H_0^1(\Omega(t))), v(0) \in H_0^1(\Omega(0)) \right\} \\ \phi_k \in X_k^0 &= \left\{ v \in L^2(I, H_0^1(\Omega(t))) \;\middle|\; (v \circ T_m)_{|I_m} \in P_0(I_m, H_0^1(\Omega(t))), v(0) \in H_0^1(\Omega(0)) \right\}. \end{aligned} \tag{10}$$

Note that the outer domain $\Omega(t)$ is not assumed to be fixed anymore.

By T_m we denote an arbitrary transformation from a reference domain $\hat{\Omega}^m$ to the space-time domain Q^m that maps $\hat{\Gamma}^m$ to $\Gamma(t)$, $\hat{\Omega}_1^m$ onto $\Omega_1(t)$ and $\hat{\Omega}_2^m$ onto $\Omega_2(t)$. In this work, we choose the domain at the new time step $\hat{\Omega}^m = \Omega(t_m)$ as reference domain. Other choices, e.g. $\hat{\Omega}^m = \Omega(t_{m-1})$ would be possible, as well. For $j = 1, ..., M$, we denote the space-time slabs in the reference system by $\hat{Q}^j := \hat{\Omega}^j \times I_j$, the space-time slabs corresponding to the subdomains ($i = 1, 2$) by $\hat{Q}_i^j := \hat{\Omega}_i^j \times I_j$

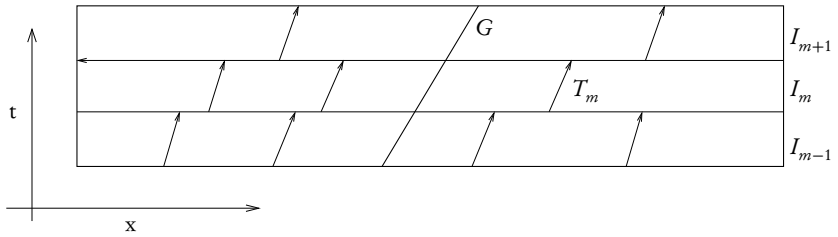

Figure 3. Illustration of the modified Galerkin trial spaces X_k^0, X_k^1. The functions $v_k \in X_k^0, X_k^1$ are polynomial on trajectories that stay within each subdomain Q_i, $i = 1,2$.

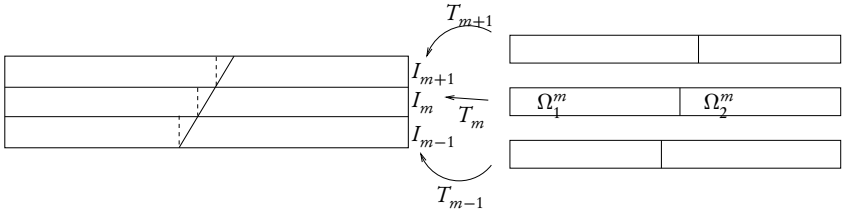

Figure 4. Piecewise definition of maps T_m. The reference domain (right sketch) corresponds to the *new* domain Ω^m and changes in each time step.

and the interface slabs by $\hat{G}^j := \hat{\Gamma}^j \times I_j$. Functions $u \in X_1^k$ and $\phi \in X_0^k$ can be written as

$$\begin{aligned}(u \circ T_m)|_{I_m} &= \frac{t - t_{m-1}}{k}(u \circ T_m)(x, t_m) + \frac{t_m - t}{k}(u \circ T_m)(x, t_{m-1}) \\ &=: \frac{t - t_{m-1}}{k}\hat{u}^m(\hat{x}) + \frac{t_m - t}{k}\hat{u}^{m-1,+}(\hat{x}) \\ (\phi \circ T_m)|_{I_m} &= \hat{\phi}^m(\hat{x})\end{aligned}$$

with $\hat{u}^m, \hat{\phi}^m, \hat{u}^{m-1,+} \in H_0^1(\hat{\Omega}^m)$ and $\hat{x} = T_m^{-1}(x,t)$. Due to the continuity condition in X_k^1, it must hold that

$$\left(\hat{u}^{m-1,+} \circ T_m^{-1}\right)(t_{m-1}) = \hat{u}^{m-1}. \tag{11}$$

In order to simplify notation, we will often skip the second superscript and use the notation $\hat{u}^{m-1}$ instead of $\hat{u}^{m-1,+}$ in $\hat{Q}^m$.

Finally, we denote by $F_m = \nabla T_m$ the spatial derivative of the transformation and by $J_m = \det(F_m)$ its determinant. We define the following bilinear form in a time interval I_m, formulated both in Eulerian coordinates on Q^m and on the reference domain $\hat{Q}^m$ in ALE coordinates:

$$\begin{aligned}B^m(u,\phi) &:= (\partial_t u, \phi)_{Q^m} + (\kappa \nabla u, \nabla \phi)_{Q^m} \\ &= \left(J_m \partial_t \hat{u} - \partial_t T_m (J_m F_m)^{-T} \hat{\nabla}_m \hat{u}, \hat{\phi}\right)_{\hat{Q}^m} + \left(\hat{\kappa}(J_m F_m)^{-T} \hat{\nabla}_m \hat{u}, F_m^{-T} \hat{\nabla}_m \hat{\phi}\right)_{\hat{Q}^m}.\end{aligned} \tag{12}$$

Here, the notation $\hat{\nabla}_m$ denotes the gradient with respect to the coordinates $\hat{x}_m$ on the reference domain $\hat{\Omega}^m$. For better readability, we will often skip the subscripts m if there is no risk for ambiguity. Comparing (6), it holds that

$$B(u,\phi) = \sum_{m=1}^{M} B^m(u,\phi) + (u(0), \phi(0))_{\Omega(0)}.$$

The discrete formulation in the trial and test spaces defined in (10) reads: Find $u_k \in X_k^1$ such that

$$B(u_k, \phi_k) = (f, \phi_k)_Q + (u^0, \phi(0))_{\Omega(0)} \quad \forall \phi_k \in X_k^0. \tag{13}$$

This formulation splits into the time-stepping scheme

$$B^m(u_k, \phi_k) = \left(J\hat{f}, \hat{\phi}_k\right)_{\hat{Q}^m} \tag{14}$$

where

$$\begin{aligned} B^m(u_k, \phi_k) := & \frac{1}{k}\left(J(\hat{u}_k^m - \hat{u}_k^{m-1}), \hat{\phi}_k^m\right)_{\hat{Q}^m} \\ & - \left(\partial_t T J F^{-T}\left(\frac{t - t_{m-1}}{k}\hat{\nabla}\hat{u}_k^m + \frac{t_m - t}{k}\hat{\nabla}\hat{u}_k^{m-1}\right), \hat{\phi}_k^m\right)_{\hat{Q}^m} \\ & + \left(\hat{\kappa} J F^{-T}\left(\frac{t - t_{m-1}}{k}\hat{\nabla}\hat{u}_k^m + \frac{t_m - t}{k}\hat{\nabla}\hat{u}_k^{m-1}\right), F^{-T}\hat{\nabla}\hat{\phi}_k^m\right)_{\hat{Q}^m}. \end{aligned} \tag{15}$$

In practice, the interface and boundary movement are often implicitly defined by the solution variables and might thus be available only at the time points t_{m-1} and t_m. To deal with this kind of problems, we want to use a further simplification of (13). We use approximations of the form

$$a(t)b(t) \approx \frac{1}{4}(a(t_m) + a(t_{m-1}))(b(t_m) + b(t_{m-1}))$$

and use the notation $\overline{J}_m = \frac{1}{2}\left(J_m(t_m) + J_m(t_{m-1})\right)$ and analogously $\overline{JF}_m^{-T}$, $\overline{F}_m^{-T}$ and $\overline{\partial_t T}_m$. Again, we will skip the subscript m if there is no risk for ambiguity. We define the discrete bilinear forms

$$\begin{aligned} B_k^m(u, \phi) &= \left(\overline{J}\partial_t \hat{u}, \hat{\phi}\right)_{\hat{Q}^m} - \left(\overline{\partial_t T}\,\overline{JF}^{-T}\hat{\nabla}\hat{u}, \hat{\phi}\right)_{\hat{Q}^m} + \left(\hat{\kappa}\overline{JF}^{-T}\hat{\nabla}\hat{u}, \overline{F}^{-T}\hat{\nabla}\hat{\phi}\right)_{\hat{Q}^m}, \\ B_k(u, \phi) &= \sum_{m=1}^{M} B_k^m(u, \phi) + (u(0), \phi(0))_{\Omega(0)}. \end{aligned}$$

We will show below that this approximation of the bilinear form $B(\cdot, \cdot)$ is of second order and will thus not perturb the overall accuracy. For $u_k \in X_k^1$ and $\phi_k \in X_k^0$, it holds that

$$\begin{aligned} B_k^m(u_k, \phi_k) = & \frac{1}{k}\left(\overline{J}\left(\hat{u}_k^m - \hat{u}_k^{m-1}\right), \hat{\phi}_k^m)\right)_{\hat{Q}^m} - \frac{1}{2}\left(\overline{\partial_t T}\,\overline{JF}^{-T}\hat{\nabla}\left(\hat{u}_k^m + \hat{u}_k^{m-1}\right), \hat{\phi}_k^m\right)_{\hat{Q}^m} \\ & + \frac{1}{2}\left(\hat{\kappa}\overline{JF}^{-T}\hat{\nabla}\left(\hat{u}_k^m + \hat{u}_k^{m-1}\right), \overline{F}^{-T}\hat{\nabla}\hat{\phi}_k^m\right)_{\hat{Q}^m}. \end{aligned}$$

The corresponding discrete variational formulation reads: Find $u_k \in X_k^1$ such that

$$B_k(u_k, \phi_k) = (f, \phi_k)_Q + (u^0, \phi_k(0))_{\Omega(0)} \quad \forall \phi_k \in X_k^0. \tag{16}$$

As the continuous solution u fulfills

$$B(u, \phi_k) = (f, \phi_k)_Q + (u^0, \phi_k^0)_{\Omega(0)} \quad \forall \phi_k \in X_k^0,$$

we have the Galerkin orthogonality

$$B(u, \phi_k) - B_k(u_k, \phi_k) = 0 \quad \forall \phi_k \in X_k^0. \tag{17}$$

Remark 2.1 (Fixed-mesh ALE)**.** *The resulting time-stepping scheme can be considered a variant of the Fixed-mesh ALE method[6]. There are two peculiarities that have not been used within the Fixed-Mesh-ALE method yet: The first one lies in the approximation of the quantities J, F and $\partial_t T$ related to the transformation. Secondly, to fit into this framework, we define $u_k^{m-1,+}$ by the projection of the residual*

$$B_{old}^m(u_k^{m-1,+}, \phi) = B_{old}^{m-1}(u_k^{m-1,-}, \phi) \quad \forall \phi \in H_0^1(\Omega(t_{m-1})) \tag{18}$$

where

$$B_{old}^m(w, \phi) := \left(-\bar{J}\hat{w} + \frac{k}{2}\overline{\partial_t T J F^{-1}}^T \hat{\nabla}\hat{w}, \hat{\phi} \right)_{\hat{\Omega}^m} + \frac{k}{2}\left(\hat{\kappa}\overline{JF}^{-T}\hat{\nabla}\hat{w}, \overline{F}^{-T}\hat{\nabla}\hat{\phi} \right)_{\hat{\Omega}^m}.$$

For our practical implementation that avoids the calculation of such a projection, see Section 4.2.

3 A priori error estimates

We will make the following regularity assumptions for the domain movement T_m.

Assumption 3.1. – *For every interval I_m, there exists a map $T_m : \hat{\Omega}^m \times I_m \to \Omega(t)$ such that for $t \in I_m$*

$$T_m(\hat{\Omega}_i^m, t) = \Omega_i(t) \quad (i = 1, 2), \qquad T_m(\hat{\Gamma}^m, t) = \Gamma(t).$$

– *Furthermore, it holds for $i = 1, 2$ that*

$$\sup_{t \in I_m} \left(\|T_m(t)\|_{W^{2,\infty}(\hat{\Omega}_i^m)} + \sum_{k=1}^{3} \|\partial_t^k T_m(t)\|_{W^{3-k,\infty}(\hat{\Omega}_i^m)} \right) \leq c$$

$$\sup_{t \in I_m} \left(\|T_m^{-1}(t)\|_{W^{2,\infty}(\hat{\Omega}_i^m)} + \sum_{k=1}^{2} \|\partial_t^k T_m^{-1}(t)\|_{W^{3-k,\infty}(\hat{\Omega}_i^m)} \right) \leq c.$$

– *Finally, we assume that T_m and $\partial_t T_m$ are continuous across the interface $\hat{\Gamma}^m$.*

Remark 3.2 (On Assumption 3.1)**.** *Assumption 3.1 implies that*

$$\sup_{t \in I_m} \|F_m(t)\|_{W^{1,\infty}(\hat{\Omega}^m)} + \sup_{t \in I_m} \|F_m^{-1}(t)\|_{W^{1,\infty}(\hat{\Omega}^m)} + \sup_{t \in I_m} \|J_m(t)\|_{W^{1,\infty}(\hat{\Omega}^m)} \leq c.$$

The latter holds true as the determinant of F_m can be written as a summed product of the entries of F_m.

Remark 3.3 (On Assumption 3.1)**.** *In many practical cases, the position of the interface and the outer boundaries depends on the solution itself and is only available at discrete points in time (e.g. by level set functions ψ^m, ψ^{m-1}). Let*

$$x^{m-1} := T_m(x^m, t_{m-1}) \in \Omega(t_{m-1}) \tag{19}$$

be the transformed coordinate corresponding to a point $x^m \in \Omega(t_m)$. Then, a suitable transformation in the interval I_m is given by

$$T_m(x^m, t) = \frac{t - t_{m-1}}{k} x^m + \frac{t_m - t}{k} x^{m-1}.$$

Here, the first time derivative is $\partial_t T_m = 1/k\,(x^m - x^{m-1})$, higher time derivatives vanish. Assumption 3.1 reduces to the boundedness of the velocity of the domain movement and its spatial derivatives.

Remark 3.4 (Construction of a mapping T_m). *Assume the interface movement is given by a vector-valued function*

$$\psi : \Gamma(t_m) \to \Gamma(t_{m-1}).$$

Such a function is available in the context of fluid-structure interactions by the Initial Point Set function (see[8] or Section 5.2), sometimes also called the Backward Characteristics method (see[7]), that traces back points to their original position in $\Omega(0)$. An extension of ψ to the complete domain $\Omega(t_m)$ (again denoted by ψ) can be obtained by e.g. a harmonic extension. Then, a transformation $T : \Omega(t_m) \to \Omega(t)$ is given by

$$T_m(x,t) = \frac{t - t_{m-1}}{k} x + \frac{t_m - t}{k} \psi(x).$$

The regularity of T_m depends only on the regularity of the boundary movement ψ and its extension at time t_m.

Remark 3.5 (Regularity). *In contrast to the ALE approach (5), we need regularity of the transformations T_m only locally in each time interval I_m. No global regularity of a mapping T is required.*

3.1 Interpolation and projection

We begin by an auxiliary result for the transformation of derivatives that we will need frequently.

Lemma 3.6. *(Transformation of derivatives) Let Assumption 3.1 be valid and $\hat{u}(\hat{x}) := (u \circ T_m^{-1})(x)$ on $\hat{Q}^m$. For $u \in H^1(Q)$, $\hat{u}$ lies piecewise in $H^1(\hat{Q}^m)$ and it holds that*

$$\left\| \hat{\nabla} \hat{u} \right\|_{\hat{Q}^m} \leq c \|\nabla u\|_{Q^m} \quad \text{and} \quad \|\partial_t \hat{u}\|_{\hat{Q}^m} \leq c \left\{ \|\partial_t u\|_{Q^m} + \|\nabla u\|_{Q^m} \right\}. \tag{20}$$

For u in $H^2\left(I, L^2(\Omega(t))\right) \cap H^1\left(I, H_0^1(\Omega(t))\right)$ it holds that

$$\left\| \partial_t^2 \hat{u} \right\|_{\hat{Q}^m} \leq c \left\{ \left\| \partial_t^2 u \right\|_{Q^m} + \|\partial_t \nabla u\|_{Q^m} + \|\nabla u\|_{Q^m} \right\}. \tag{21}$$

Proof. The proof is standard, see e.g.[17]. □

We define the interpolation $i_k u$ as standard nodal interpolant in each reference space-time slab $\hat{Q}^m$. This is equivalent to setting

$$i_k u(t_m) = u(t_m) \quad \forall m = 1, ..., M$$

in each time-grid point t_m.

Lemma 3.7. *Assume Assumption 3.1. If $u \in H^2(Q_1 \cup Q_2)$, it holds for the interpolation error that*

$$\left\| \partial_t^l (u - i_k u) \right\|_Q \leq c k^{2-l} \left\{ \left\| \partial_t^2 u \right\|_{Q_1 \cup Q_2} + \|\partial_t \nabla u\|_{Q_1 \cup Q_2} + \|\nabla u\|_Q \right\}. \tag{22}$$

for $l = 0, 1$.

Proof. We begin with the case $l = 0$ and transform to the reference domain where we use a standard estimate. The determinant J is bounded by Assumption 3.1

$$\|u - i_k u\|_{Q^m}^2 = \left\| J^{1/2} \left(\hat{u} - \widehat{i_k u} \right) \right\|_{\hat{Q}^m}^2 \leq \left(\sup_{t \in I_m} \|J\|_{\infty, \hat{\Omega}^m} \right) \|\hat{u} - i_k \hat{u}\|_{\hat{Q}^m}^2 \leq c k^4 \|\partial_t^2 \hat{u}\|_{\hat{Q}_1^m \cup \hat{Q}_2^m}^2$$

Transformation of derivatives (see Lemma 3.6), summation over $m = 1, ..., M$ and taking the square root complete the proof. The case $l = 1$ follows analogously by using

$$\|\partial_t(u - i_k u)\|^2_{Q^m} \leq c\,\|\partial_t(\hat{u} - i_k\hat{u})\|^2_{\hat{Q}^m} + \left\|\hat{\nabla}(\hat{u} - i_k\hat{u})\right\|^2_{\hat{Q}^m} \leq ck^2\left(\left\|\partial_t^2\hat{u}\right\|^2_{\hat{Q}^m} + \left\|\partial_t\hat{\nabla}\hat{u}\right\|^2_{\hat{Q}^m}\right).$$

□

Remark 3.8. *Even in the case of a fixed outer boundary $\partial\Omega(t)$, an analogous interpolation estimate is not possible for an interpolant in the space $\hat{X}^1_k$ if the interface $\Gamma(t)$ is moving.*

Next, we prove a lemma that estimates the interpolation error within the discrete bilinear form.

Lemma 3.9. *Let $u \in \mathcal{H}^{2,1} \cap \mathcal{H}^{1,2}$. For $\phi_k \in X^0_k$, it holds under Assumption 3.1 that*

$$B_k(u - i_k u, \phi_k) \leq ck^2\left(\|\partial_t^2\nabla u\|_Q + \|\partial_t\nabla^2 u\|_Q + \|\nabla^2 u\|_Q\right)\|\nabla\phi_k\|_Q. \tag{23}$$

Proof. We write $\eta_k = u - i_k u$. By definition, we have on each space-time slab

$$B^m_k(\eta_k, \phi_k) = (\bar{J}\partial_t\hat{\eta}_k, \hat{\phi}_k)_{\hat{Q}^m} - \left(\overline{\partial_t T JF}^{-T}\hat{\nabla}\hat{\eta}_k, \hat{\phi}^m_k\right)_{\hat{Q}^m} + \left(\hat{\kappa}\overline{JF}^{-T}\hat{\nabla}\hat{\eta}_k, \overline{F}^{-T}\hat{\nabla}\hat{\phi}^m_k\right)_{\hat{Q}^m}.$$

The first part vanishes as $\hat{\phi}_k$ is piecewise constant and $\eta_k(t_j) = 0$ for a time grid point t_j

$$(\bar{J}\partial_t\hat{\eta}_k, \hat{\phi}_k)_{\hat{Q}^m} = -(\bar{J}\hat{\eta}_k, \partial_t\hat{\phi}_k)_{\hat{Q}^m} + (\bar{J}\hat{\eta}_k(t_m), \hat{\phi}_k)_{\hat{\Omega}^m} - (\bar{J}\hat{\eta}_k(t_{m-1}), \hat{\phi}_k)_{\hat{\Omega}^m} = 0.$$

For the remaining terms, we apply the Cauchy-Schwarz inequality and use Assumption 3.1

$$B^m_k(\eta_k, \phi_k) \leq C\left\|\hat{\nabla}\hat{\eta}_k\right\|_{\hat{Q}^m}\left\|\hat{\nabla}\hat{\phi}^m_k\right\|_{\hat{Q}^m} \leq C\,\|\nabla\eta_k\|_{Q^m}\,\|\nabla\phi_k\|_{Q^m}.$$

Summation over $m = 1, ..., M$ and Lemma 3.7 gives the statement (23).

□

Finally, we define a projection into the space of piecewise constant functions by setting in each time interval I_m

$$P^0_k : X \to X^0_k, \qquad \left(P^0_k v \circ T_m\right)|_{I_m} = \frac{1}{2}\left(\hat{v}(t_m) + \hat{v}(t_{m-1})\right). \tag{24}$$

3.2 Error between discrete and continuous bilinear forms

Next, we provide a result that estimates the difference between the bilinear forms $B(\cdot,\cdot)$ and $B_k(\cdot,\cdot)$. Before, we provide an auxiliary result that will be needed to deal with the domain movement.

Lemma 3.10. *Let $a, b \in W^{1,\infty}(I, L^\infty(\Omega(t)))$ and define a function $\overline{a}$ by $\overline{a} = 1/2(a(t_m) + a(t_{m-1}))$. For arbitrary functions $f, g \in L^2(\hat{\Omega}^m)$ and $t_i \in I_m$, it holds that*

$$\left((a(t_i) - \overline{a})f, g\right)_{\hat{Q}^m} \leq ck\left|(f, g)_{\hat{Q}^m}\right|, \tag{25}$$

$$\left((a - \overline{a})f, g\right)_{\hat{Q}^m} \leq ck\left|(f, g)_{\hat{Q}^m}\right|, \tag{26}$$

$$\left((a(t)b(t) - \overline{a}\,\overline{b})f, g\right)_{\hat{Q}^m} \leq ck\|f\|_{\hat{Q}^m}\|g\|_{\hat{Q}^m}. \tag{27}$$

For $g \in X_k^0$ piecewise constant, $f \in H^1(Q)$ and $a, b \in W^{2,\infty}(I, L^\infty(\Omega(t)))$, it holds that

$$((a(t)-\overline{a})f, g)_{\hat{Q}^m} \leq ck^2 \|f\|_{H^1(I_m, L^2(\hat{\Omega}^m))} \|g\|_{\hat{Q}^m}, \tag{28}$$

$$\left((a(t)b(t)-\overline{a}\,\overline{b})f, g\right)_{\hat{Q}^m} \leq ck^2 \|f\|_{H^1(I_m, L^2(\hat{\Omega}^m))} \|g\|_{\hat{Q}^m}. \tag{29}$$

Similar results hold true for vector-valued functions.

Proof. The estimates (25) to (27) follow by simple interpolation arguments. To show (28), we add $\pm\overline{f}$

$$((a(t)-\overline{a})f, g))_{\hat{Q}^m} = \left((a(t)-\overline{a})(f-\overline{f}), g)\right)_{\hat{Q}^m} + \left((a(t)-\overline{a})\overline{f}, g)\right)_{\hat{Q}^m}. \tag{30}$$

We estimate the first term by using the Hölder inequality

$$\begin{aligned}\left((a(t)-\overline{a})(f-\overline{f}), g)\right)_{\hat{Q}^m} &\leq \sup_{t\in I_m} \|a-\overline{a}\|_{\infty,\hat{\Omega}^m} \|f-\overline{f}\|_{\hat{Q}^m} \|g\|_{\hat{Q}^m} \\ &\leq ck^2 \sup_{t\in I_m} \|\partial_t a\|_{\infty,\hat{\Omega}^m} \|\partial_t f\|_{\hat{Q}^m} \|g\|_{\hat{Q}^m}.\end{aligned} \tag{31}$$

For the second term, we notice that neither $\overline{f}$ nor g depend on time and thus, time integration reduces to an error estimate for the trapezoidal rule for a

$$\left((a(t)-\overline{a})\overline{f}, g)\right)_{\hat{Q}^m} = \int_{\hat{\Omega}^m} \overline{f}\, g \int_{I_m} (a(t)-\overline{a})\,\mathrm{d}t \leq ck^2 \sup_{t\in I_m} \|\partial_t^2 a\|_{\infty,\hat{\Omega}^m} \|\overline{f}\|_{\hat{Q}^m} \|g\|_{\hat{Q}^m}. \tag{32}$$

The term including $\overline{f}$ can be estimated by

$$\|\overline{f}\|_{\hat{Q}^m} \leq \|f-\overline{f}\|_{\hat{Q}^m} + \|f\|_{\hat{Q}^m} \leq ck \|\partial_t f\|_{\hat{Q}^m} + \|f\|_{\hat{Q}^m}. \tag{33}$$

The estimates(30) to (33) imply (28). To show (29), we use a similar argumentation and split the corresponding first term into

$$\begin{aligned}\sup_{x\in\hat{\Omega}^m} \left(\int_{I_m} a(t)b(t) - \overline{a}\,\overline{b}\,\mathrm{d}t \right) = \sup_{x\in\hat{\Omega}^m} \Big(&\int_{I_m} (a(t)-\overline{a}) \left(b(t)-\overline{b}\right) \mathrm{d}t \\ &+ \int_{I_m} (a(t)-\overline{a})\,\overline{b}\,\mathrm{d}t + \int_{I_m} \overline{a}\left(b(t)-\overline{b}\right)\mathrm{d}t \Big).\end{aligned}$$

□

Lemma 3.11. *Let Assumption 3.1 be valid. For $u \in H^2(Q_1 \cup Q_2)$ and $z_k \in X_k^0$ it holds that ($m = 1, ..., M$)*

$$\begin{aligned}\left|B^m(u, z_k) - B_k^m(u, z_k)\right| &\leq ck^2 \|\hat{u}\|_{H^2(\hat{Q}_1^m \cup \hat{Q}_2^m)} \|\hat{\nabla}\hat{z}_k\|_{\hat{Q}}^m \\ &\leq ck^2 \|u\|_{H^2(Q_1^m \cup Q_2^m)} \|\nabla z_k\|_Q^m\end{aligned} \tag{34}$$

and

$$\left|B(u, z_k) - B_k(u, z_k)\right| \leq ck^2 \|u\|_{H^2(Q_1 \cup Q_2)} \|\nabla z_k\|_Q. \tag{35}$$

Proof. By definition, we have

$$B^m(u,z_k)-B_k^m(u,z_k)=\left((J-\bar{J})\partial_t\hat{u}-\left(\partial_t TJF^{-T}-\overline{\partial_t T}\,\overline{JF}^{-T}\right)\hat{\nabla}\hat{u},\hat{z}_k^m\right)_{\hat{Q}^m}$$
$$+\left(\hat{\kappa}\left(JF^{-1}F^{-T}-\overline{JF}^{-1}\overline{F}^{-T}\right)\hat{\nabla}\hat{u},\hat{\nabla}\hat{z}_k^m\right)_{\hat{Q}^m}. \tag{36}$$

We estimate the integrals on the domains $\hat{Q}_1^m$ and $\hat{Q}_2^m$ separately. Applying (28) for the determinant J, the first term in (36) is bounded by

$$\left((J-\bar{J})\partial_t\hat{u},\hat{z}_k^m\right)_{\hat{Q}^m}\leq ck^2\left(\|\partial_t^2\hat{u}\|_{\hat{Q}_1^m}+\|\partial_t^2\hat{u}\|_{\hat{Q}_2^m}\right)\|\hat{z}_k^m\|_{\hat{Q}^m}.$$

Similarly, we get for the remaining terms in (36) using the Poincaré inequality

$$\left(\hat{\kappa}(JF^{-T}F^{-1}-\overline{JF}^{-T}\overline{F}^{-1})\hat{\nabla}\hat{u},\hat{\nabla}\hat{z}_k^m\right)_{\hat{Q}^m}-\left((\partial_t TJF^{-T}-\overline{\partial_t T}\,\overline{JF}^{-T})\hat{\nabla}\hat{u},\hat{z}_k^m\right)_{\hat{Q}^m}$$
$$\leq ck^2\left(\|\partial_t\hat{\nabla}\hat{u}\|_{\hat{Q}_1^m}+\|\partial_t\hat{\nabla}\hat{u}\|_{\hat{Q}_2^m}\right)\|\hat{\nabla}\hat{z}_k^m\|_{\hat{Q}^m}.$$

Transformation of derivatives (Lemma 3.6) yields (34). (35) follows by summation over $m=1,\dots,M$. □

3.3 Error estimates

Our error estimates will be based on the following lemma.

Lemma 3.12 (Discrete Gronwall lemma)**.** *Let $(w_n)_{n\geq 0},(p_n)_{n\geq 0},(a_n)_{n\geq 0}$ and $(b_n)_{n\geq 0}$ be sequences of non-negative numbers and $c_0\geq 0$. Furthermore, let the inequality*

$$w_M+\sum_{n=1}^{M}p_n\leq\sum_{n=1}^{M}(a_nw_n+b_n)+c_0$$

be valid for all $n\geq 0$. For $\sigma_M=1-a_M>0$, it holds that

$$w_M+\sum_{n=1}^{M}p_n\leq\exp\left(\sigma_M^{-1}\sum_{n=1}^{M}a_n\right)\left(c_0+\sum_{n=1}^{M}b_n\right).$$

A proof for this result can be found e.g. in [14]. Our first theorem estimates the error $u-u_k$ at a time grid point t_m.

Theorem 3.13. *Let $u\in X$ be the solution of (6), $u_k\in X_k^1$ the time discrete solution of (16) and $e_k=u-u_k$. Furthermore, let $f\in\mathscr{H}^{2,0}\cap\mathscr{H}^{1,2}\cap\mathscr{H}^{0,4}$, $u^0\in H^6(\Omega_1(0)\cup\Omega_2(0))$, Q_1 and Q_2 sufficiently smooth and let u^0 satisfy the compatibility conditions such that the regularity estimate (3) is fulfilled. Under Assumption 3.1, it holds that*

$$\|e_k(t_m)\|_{\Omega(t_m)}\leq ck^2\exp(ct_m)\left(\sum_{k=0}^{2}\|f\|_{k,2(m-k)}+\|u^0\|_{H^6(\Omega_1(0)\cup\Omega_2(0))}\right). \tag{37}$$

Proof. We start with the Galerkin orthogonality (17)

$$B(u,\phi_k)-B_k(u_k,\phi_k)=0\quad\forall\phi_k\in X_k^0$$

and write again $\eta_k = u - i_k u$ for the interpolation error and $\xi_k = i_k u - u_k$. With the Galerkin orthogonality it follows that

$$B_k(\xi_k, \phi_k) = B_k(u, \phi_k) - B(u, \phi_k) - B_k(\eta_k, \phi_k) \quad \forall \phi_k \in X_k^0. \tag{38}$$

We test (38) with $\phi_k = P_k^0 e_k = P_k^0 \xi_k$ which means $\hat{\phi}^m = \frac{1}{2}(\hat{e}_k^m + \hat{e}_k^{m-1})$ and get on every time interval I_m:

$$\begin{aligned} \frac{1}{2k}(\bar{J}(\hat{e}_k^m - \hat{e}_k^{m-1}), \hat{e}_k^m + \hat{e}_k^{m-1})_{\hat{Q}^m} - \frac{1}{4}\left(\overline{\partial_t T}\,\overline{JF}^{-T}(\hat{\nabla}\hat{e}_k^m + \hat{\nabla}\hat{e}_k^{m-1}), \hat{e}_k^m + \hat{e}_k^{m-1}\right)_{\hat{Q}^m} \\ + \frac{1}{4}\left(\hat{\kappa}\overline{JF}^{-T}\hat{\nabla}(\hat{e}_k^m + \hat{e}_k^{m-1}), \overline{F}^{-T}\hat{\nabla}(\hat{e}_k^m + \hat{e}_k^{m-1})\right)_{\hat{Q}^m} \\ = B_k^m(u, P_k^0 e_k) - B^m(u, P_k^0 e_k) - B_k^m(\eta_k, P_k^0 e_k). \end{aligned} \tag{39}$$

Before we estimate (39) term by term, note that with the help of Lemma 3.10 and Assumption 3.1, we have for an arbitrary function $f \in L^2(\Omega(t_i))$, $i = m-1$ or $i = m$ and its counterpart $\hat{f} \in L^2(\hat{\Omega}^m)$

$$\begin{aligned} \left\|\bar{J}^{1/2}\hat{f}\right\|_{\hat{\Omega}^m}^2 = \left(\bar{J}\hat{f}, \hat{f}\right)_{\hat{\Omega}^m} &= \left(J(t_i)\hat{f}, \hat{f}\right)_{\hat{\Omega}^m} + \left(\left(\bar{J} - J(t_i)\right)\hat{f}, \hat{f}\right)_{\hat{\Omega}^m} \\ &\geq \left\|J(t_i)^{1/2}\hat{f}\right\|_{\hat{\Omega}^m}^2 - ck\left\|\hat{f}\right\|_{\hat{\Omega}^m}^2 \\ &\geq (1-ck)\left\|J(t_i)^{1/2}\hat{f}\right\|_{\hat{\Omega}^m}^2 = (1-ck)\|f\|_{\Omega(t_i)}^2. \end{aligned}$$

The same argumentation can be used e.g. for F^{-T} instead of J. We get for the first term in (39)

$$\begin{aligned} \frac{1}{2k}(\bar{J}(\hat{e}_k^m - \hat{e}_k^{m-1}), \hat{e}_k^m + \hat{e}_k^{m-1})_{\hat{Q}^m} &= \frac{1}{2}\left\|\bar{J}^{1/2}\hat{e}_k^m\right\|_{\hat{\Omega}^m}^2 - \frac{1}{2}\left\|\bar{J}^{1/2}\hat{e}_k^{m-1}\right\|_{\hat{\Omega}^m}^2 \\ &\geq \left(\frac{1}{2} - ck\right)\|e_k(t_m)\|_{\Omega(t_m)}^2 - \left(\frac{1}{2} + ck\right)\left\|e_k(t_{m-1})\right\|_{\Omega(t_{m-1})}^2. \end{aligned}$$

For the second term we use Assumption 3.1, Lemma 3.10 and Young's inequality and obtain

$$\begin{aligned} &\frac{1}{4}(\overline{\partial_t T}\,\overline{JF}^{-T}\hat{\nabla}(\hat{e}_k^m + \hat{e}_k^{m-1}), \hat{e}_k^m + \hat{e}_k^{m-1})_{\hat{Q}^m} \\ &\quad \geq -c\left\|\overline{JF}^{-T}\hat{\nabla}(\hat{e}_k^m + \hat{e}_k^{m-1})\right\|_{\hat{Q}^m}\left\|\hat{e}_k^m + \hat{e}_k^{m-1}\right\|_{\hat{Q}^m} \\ &\quad \geq -c\|JF^{-T}\hat{\nabla}(\hat{e}_k^m + \hat{e}_k^{m-1})\|_{\hat{Q}^m} k^{1/2}\left(\|\hat{e}_k^m\|_{\hat{\Omega}^m} + \|\hat{e}_k^{m-1}\|_{\hat{\Omega}^m}\right) \\ &\quad \geq -\frac{\kappa_{\min}}{8}\|\nabla P_k^0 e_k\|_{Q^m}^2 - ck\left(\|e_k^m\|_{\Omega(t_m)}^2 + \|e_k^{m-1}\|_{\Omega(t_{m-1})}^2\right). \end{aligned}$$

With similar arguments we get for the third term

$$\frac{1}{4}\left(\hat{\kappa}\overline{JF}^{-T}\hat{\nabla}(\hat{e}_k^m + \hat{e}_k^{m-1}), \overline{F}^{-T}\hat{\nabla}(\hat{e}_k^m + \hat{e}_k^{m-1})\right)_{\hat{Q}^m} \geq (1-ck)\kappa_{\min}\|\nabla P_k^0 e_k\|_{Q^m}^2.$$

For the first part on the right-hand side of (39), we use Lemma 3.11 and Young's inequality

$$B_k^m(u, P_k^0 e_k) - B^m(u, P_k^0 e_k) \leq ck^2\|u\|_{H^2(Q_1^m \cup Q_2^m)}\|\nabla P_k^0 e_k\|_{Q^m}^2 \leq ck^4\|u\|_{H^2(Q_1^m \cup Q_2^m)}^2 + \frac{\kappa_{\min}}{8}\|\nabla P_k^0 e_k\|_{Q^m}^2.$$

For the second part, it follows with Lemma 3.9

$$B_k^m(\eta_k, P_k^0 e_k) \leq ck^4\left(\|\partial_t^2 \nabla u\|_{Q_1^m \cup Q_2^m}^2 + \|\partial_t \nabla^2 u\|_{Q_1^m \cup Q_2^m}^2 + \|\nabla^2 u\|_Q^2\right) + \frac{\kappa_{\min}}{8}\|\nabla P_k^0 e_k\|_{Q^m}^2$$

Altogether we have shown that

$$\begin{aligned}\left\|e_k(t_m)\right\|^2_{\Omega(t_m)} - \left\|e_k(t_{m-1})\right\|^2_{\Omega(t_{m-1})} + \frac{\kappa_{\min}}{4}\left\|\nabla P_k^0 e_k\right\|^2_{Q^m} \\ \leq ck\left\{\|e_k(t_m)\|^2_{\Omega(t_m)} + \left\|e_k(t_{m-1})\right\|^2_{\Omega(t_{m-1})}\right\} \\ + ck^4\left(\|\partial_t^2\nabla u\|_{Q_1^m\cup Q_2^m} + \|\partial_t\nabla^2 u\|_{Q_1^m\cup Q_2^m} + \|u\|^2_{H^2(Q_1^m\cup Q_2^m)}\right).\end{aligned}$$

Finally, summation over m and the regularity estimate (3) yield

$$\begin{aligned}\|e_k(T)\|^2_{\Omega(T)} + \frac{\kappa_{\min}}{4}\|\nabla P_k^0 e_k\|^2_Q \\ \leq c\sum_{m=1}^{M}\left(k\|e_k(t_m)\|^2_{\Omega(t_m)}\right) + ck^4\left(\sum_{k=0}^{2}\|f\|_{k,2(2-k)} + \|u^0\|_{H^6(\Omega_1(0)\cup\Omega_2(0))}\right).\end{aligned}$$

Applying the discrete Gronwall lemma (Lemma 3.12) and using the regularity estimate (3) prove the assertion. □

Next, we show a similar result for the space-time L^2 norm:

Theorem 3.14. *Let $u \in X$ be the solution of (6), $u_k \in X_k^1$ the time discrete solution of (16) and $e_k = u - u_k$. Under the conditions of Theorem 3.13, it holds that*

$$\|e_k\|_Q \leq ck^2\exp(cT)\left(\sum_{k=0}^{2}\|f\|_{k,2(m-k)} + \|u^0\|_{H^6(\Omega_1(0)\cup\Omega_2(0))}\right). \tag{40}$$

Proof. We split the error e_k again into an interpolation error $\eta_k = u - i_k u$ and a discrete part $\xi_k = i_k u - u_k$

$$\|e_k\|_Q \leq \|\eta_k\|_Q + \|\xi_k\|_Q.$$

The interpolation error is bounded by Lemma 3.7

$$\|\eta_k\|_Q \leq ck^2\|u\|_{H^2(Q_1\cup Q_2)}.$$

For the discrete part, note that $\xi_k(t_m) = e_k(t_m)$ and thus the result of Theorem 3.13 is valid for ξ_k as well. By definition, we have

$$\begin{aligned}\|\xi_k\|^2_{Q^m} = \int_{\hat{Q}^m} J\left(\frac{t-t_{m-1}}{k}\hat{\xi}_k(t_m) + \frac{t_m - t}{k}\hat{\xi}_k(t_{m-1})\right)^2 d\hat{x}\,dt \\ \leq 2(1+ck)\left(\|J(t_m)\hat{\xi}_k(t_m)\|^2_{\hat{Q}^m} + \|J(t_{m-1})\hat{\xi}_k(t_{m-1})\|^2_{\hat{Q}^m}\right) \\ \leq ck\left(\|\xi_k(t_m)\|^2_{\Omega(t_m)} + \|\xi_k(t_{m-1})\|^2_{\Omega(t_{m-1})}\right).\end{aligned}$$

We sum over all time intervals $m = 1,\ldots,M$, use Theorem 3.13 and $M = T/k$ to get

$$\|\xi_k\|^2_Q \leq \sum_{m=1}^{M} ck\|\xi_k(t_m)\|^2_{\Omega(t_m)} \leq ck^4\exp(cT)\left(\sum_{k=0}^{2}\|f\|_{k,2(m-k)} + \|u^0\|_{H^6(\Omega_1(0)\cup\Omega_2(0))}\right).$$

□

3.4 On the regularity of the data

The regularity for the data f and u^0 on the right-hand side in the Theorems 3.13 and 3.14 is not optimal. Instead, the estimate

$$\|e_k\| \leq ck^2 \exp(cT) \left(\sum_{k=0}^{1} \|f\|_{k,2(m-k)} + \|u^0\|_{H^4(\Omega_1(0)\cup\Omega_2(0))} \right).$$

is possible for both norms by a more involved argumentation. The necessity for the higher regularity for the data in the argumentation above comes from Lemma 3.9. There, we estimated the diffusive term by

$$(\hat{\kappa}\overline{JF}^{-T}\hat{\nabla}\hat{\eta}_k, \overline{F}^{-T}\hat{\nabla}\widehat{P_k^0 e_k})_{\hat{Q}^m} \leq C\|\nabla\eta_k\|_{Q^m}\|\nabla P_k^0 e_k\|_{Q^m}. \tag{41}$$

and used a bound for $\|\nabla\eta_k\|_{Q^m}$ that depends on the term $\|\partial_t^2\nabla u\|$ which by (3) requires higher regularity of the data. To avoid this, one could think of applying integration by parts for the left-hand side in (41). Then, however, we would need a stability bound for

$$\overline{\Delta}P_k^0 e_k := \widehat{\operatorname{div}}\left(\overline{F}^{-1}\overline{JF}^{-T}\hat{\nabla}\widehat{P_k^0 e_k}\right).$$

This is possible in the case of a fixed interface by a similar argumentation as in the proof of Theorem 3.13. In the case of a moving interface, we have the additional terms

$$B_k^m(\eta_k, \overline{\Delta}P_k^0 e_k) \quad \text{and} \quad \left(\left[\overline{\Delta}P_k^0 e_k, \hat{n}(\hat{\kappa}\overline{F}^{-1}\overline{JF}^{-T}\hat{\nabla}\widehat{P_k^0 e_k})\right] \right)_{\hat{\Gamma}^m}$$

when testing (39) by $\overline{\Delta}P_k^0 e_k$. We do not see any way to estimate these terms by an appropriate bound to show the desired stability estimate. To circumvent the necessity for higher regularity of the data, there is another possibility, however. Therefore, we define $z_k \in X_k^0$ as solution to the discrete dual problem

$$B_k(\phi_k, z_k) = (e_k, \phi_k) \quad \forall \phi_k \in X_k^1.$$

By using Galerkin orthogonality, this yields

$$(e_k, \xi_k) = B_k(\xi_k, z_k) = B_k(i_k u, z_k) - B(u, z_k) = B_k(u, z_k) - B(u, z_k) - B_k(\eta_k, z_k). \tag{42}$$

The only difficult term to estimate is again the diffusive part of $B_k(\eta_k, z_k)$. In contrast to the situation above, we have z_k instead of $P_k^0 e_k$ in (42). The advantage of this situation is now that to z_k, there is a corresponding continuous counterpart z which is the dual solution to

$$B(\phi, z) = (e_k, \phi) \quad \forall \phi \in X.$$

For z integration by parts will not cause any problematic terms. Inserting $\pm z$ and using integration by parts yields

$$\begin{aligned}(\kappa\nabla\eta_k, \nabla z_k)_{Q^m} &= (\kappa\nabla\eta_k, \nabla(z_k - z))_{Q^m} + (\kappa\nabla\eta_k, \nabla z)_{Q^m} \\ &= -\left(\operatorname{div}(\kappa\nabla\eta_k), (z_k - z)\right)_{Q^m} + \left([n(t)\kappa\nabla\eta_k], z_k - z\right)_{\Gamma^m} + \left(\eta_k, \operatorname{div}(\kappa\nabla z)\right)_{Q^m}.\end{aligned}$$

It remains to derive an error estimate for the dual solutions in the L^2-norm as well as the estimation of the interface term. For the details, we refer to [11].

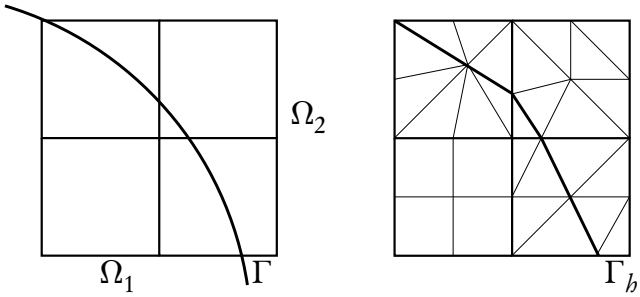

Figure 5. Left: Patches $P \in \Omega_{2h}$ with interface Γ. Right: Cells $T \in \Omega_h$ that arise from subdivision of patches $\hat{P}_1, ..., \hat{P}_4$ into eight triangles or four quadrilaterals and the piecewise linear discrete interface Γ_h.

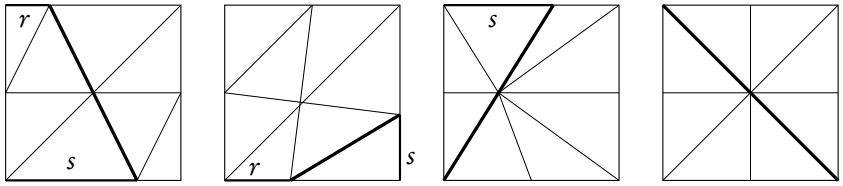

Figure 6. Different types of cut patches. From left to right: A, B, C and D. The subdivision can be anisotropic with $r, s \in (0,1)$ arbitrary.

4 Practical aspects

An important component of the numerical algorithm is the choice of a projection of the solution at the previous time step u_k^{m-1} from the old to the new reference domain. In this section, we will show that we do not need to calculate such a projection, as we can directly evaluate the arising integrals including u_k^{m-1}. Therefore, we will derive a numerical integration scheme that integrates scalar products including functions from two different reference domains exactly. We will see in Section 5 that exact integration is crucial in order to obtain second-order accuracy.

Before, we describe the integration scheme we use, we introduce a spatial discretization scheme that guarantees optimal convergence in space in Section 4.1. The time discretization scheme presented here is, however, not restricted to this spatial discretization, other choices e.g. based on the extended finite element method (XFEM, [16]), are possible.

4.1 Spatial discretization: A locally modified finite element scheme

For spatial discretization, we use the modified finite element scheme introduced in [12]. The key idea is to use one fixed background mesh consisting of patches $P \in \Omega_h^c$ for all time steps. In this way, we avoid the need for remeshing as we advance in time and the reference domain changes. Furthermore, the transition from functions defined on an old reference domain $\hat{\Omega}^{m-1}$ to the new domain $\hat{\Omega}^m$ by means of exact numerical integration will be considerably simplified (see Section 4.2).

The region for triangulation for Ω_h^c has to be chosen large enough to cover all domains $\Omega(t), t \in I$. Grid points that lie outside the reference domain $\hat{\Omega}^m$ may be eliminated from the system matrix in time step m. In order to obtain a spatial discretization of optimal order, special care has to be taken for the cells that are cut by the interface. If a patch is cut by the interface, we divide it into 8 triangles in such a way that the interface is resolved properly, see Figure 5. Furthermore, in order

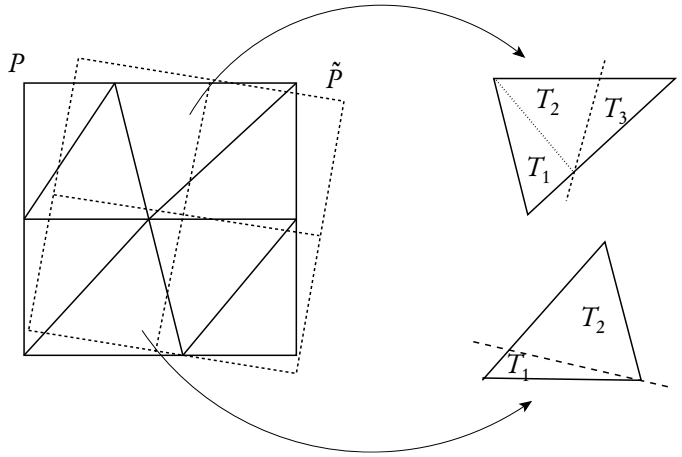

Figure 7. Left: Two overlapping elements $P \in \Omega_h^{m,c}$ and $\tilde{P} \in \tilde{\Omega}_h^{m-1,c}$. Right: A triangle can be cut by a line in two different ways: The cut goes through two edges or through an edge end a vertex. We add three or two triangles to the list $\mathscr{L}$, respectively.

to avoid hanging nodes and to have the same number of degrees of freedom independent of the interface location, we split a patch into four quadrilaterals if $P \cap \Gamma(t) = \emptyset$.

The four cases that have to be dealt with are shown in Figure 6: In all four cases, we can adjust the edge midpoints and the midpoint of the cell in such a way that the interface is resolved in a linear approximation. On the patch mesh Ω_h^c, we define the finite element trial space $V_h \subset H_0^1(\Omega)$ as an iso-parametric space. If a patch is not cut by the interface, we use the standard space of bilinear functions $\hat{Q}$ (bilinear on each of the four sub-quads) for both reference element transformation and the finite element basis. If a patch $P \in \Omega_h^c$ is cut, we use the space $\hat{Q}_{\text{mod}}$ of piecewise linear functions (linear on each of the eight triangles) for transformation and basis.

Although this ansatz is in principle equivalent to a finite element ansatz on a hybrid mesh consisting of quadrilaterals and triangles, we base our implementation on the patch mesh Ω_h^c and use whole patches $\hat{P}$ as reference elements. The local subdivision into triangles and quadrilaterals is hereby included in the local transformation

$$\hat{\xi}_P : \hat{P} \to P, \quad \hat{\xi}_P \in \hat{Q}_{\text{mod}} \quad (\text{or } \hat{Q} \text{ resp}).$$

For $m = 1, ..., M$, we obtain meshes Ω_h^m consisting of quadrilaterals and triangles that differ from each other in the interface region. The arising subcells can become arbitrarily anisotropic for $r, s \to 0, 1$ (Figure 6). We can guarantee, however, that a maximum angle condition remains valid. This enables us to show optimal error estimates of second order. Furthermore, using a hierarchical finite element basis, the condition number of the corresponding system matrix remains bounded[12].

4.2 Projection between reference domains and numerical integration

In the time-stepping scheme (16), the old solution $\hat{u}_k^{m-1}$ appears as $\hat{u}_k^{m-1,+}$ on the new reference domain $\hat{\Omega}^m$. However, from the previous time-step, $\hat{u}_k^{m-1}$ is given as a function on $\hat{\Omega}^{m-1}$. To evaluate the expressions in (16), we have to apply a projection to the new reference domain. Using interpolation may lead to a reduced order of convergence (see Section 5). A projection that conserves the order of convergence is given in (18). Here, however, we will show that it is not necessary to calculate this projection.

By definition of the trial space X_k^1, we have the continuity relation (11)

$$\hat{u}_k^{m-1,+} = \hat{u}_k^{m-1} \circ T_m^{-1}(t_{m-1}),$$

i.e. continuity in the current configuration on $\Omega(t_{m-1})$. For the derivatives, we have

$$\hat{\nabla}_m \hat{u}_k^{m-1,+} = \left(F_{m-1}^{-T}(t_{m-1})\hat{\nabla}_{m-1}\hat{u}_k^{m-1}\right) \circ T_m^{-1}(t_{m-1}).$$

In our practical implementation we use these expressions to evaluate $\hat{u}^{m-1,+}$ on the old domain $\hat{\Omega}^{m-1}$. As an example, let us consider the evaluation of

$$\int_{\hat{\Omega}^m} \hat{u}_k^{m-1,+} \cdot \hat{\phi}_k^m \,\mathrm{d}\hat{x} = \int_{\hat{\Omega}^m} \left(\hat{u}_k^{m-1} \circ T_m^{-1}(t_{m-1})\right) \cdot \hat{\phi}_k^m \,\mathrm{d}\hat{x}. \tag{43}$$

While the first factor on the right-hand side is a smooth function on the cells of the moved grid $\tilde{\Omega}_h^{m-1} = T_m^{-1}(t_{m-1})(\Omega_h^{m-1})$, the second factor is smooth on Ω_h^m (see Figure 7 for an example of two overlapping patches $P \in \Omega_h^{m,c}$ and $\tilde{P} \in \tilde{\Omega}_h^{m-1,c}$). A high-order integration formula has to account for both the singularities of the integrands. For this purpose, we construct a cut grid consisting of triangles that contains the mesh lines of both grids. In two dimensions, this cut grid can be constructed by a rather simple algorithm:

Algorithm 4.1. *We initialize a list of triangles $\mathscr{L}$ that contains the elements of $\hat{\Omega}^m$ (quadrilaterals are split into two triangles). Then, we augment the list in the following way: For all mesh lines e_i in $\tilde{\Omega}_h^{m-1}$:*

1. *Check which triangles in $\mathscr{L}$ are cut by e_i.*
2. *If a triangle is cut, eliminate the triangle from the list $\mathscr{L}$, split it into two or three subtriangles (see Figure 7) and add them to $\mathscr{L}$.*

In three space dimension, the construction of a cut grid is much more technical. We refer to Sudakhar & Wall [18] and Bastian & Engwer [4] for possible approaches. Once the list $\mathscr{L}$ has been created, we use a standard Gauß quadrature rule on the triangles in $\mathscr{L}$.

Remark 4.1. *The movement $T_m^{-1}(t_{m-1})$ of grid cells is bounded by Assumption 3.1. In our practical implementation, we make the additional assumption that the interface does not jump over more than one patch within one time step. In the opposite case, we decrease the time step $k = t_m - t_{m-1}$. In this way, we only have to check if the triangles that are part of the same patch and the neighboring patches are affected by e_i in 1.*

5 Numerical Examples

Finally, we present two numerical examples to substantiate the findings of the previous section.

5.1 Numerical example with analytical solution

We consider Problem (1) on a moving domain $\Omega(t) = \Omega_1(t) \cup \Omega_2(t) \cup \Gamma(t)$. The subdomains are defined by

$$\Omega_1(t) = [-1,1] \times [-1,t], \quad \Omega_2(t) = [-1,1] \times [t,1+t].$$

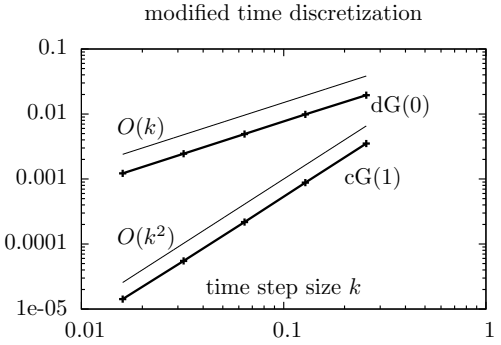

Figure 8. End time error of the modified dG(0) and cG(1) schemes for $k = h$ and a fixed outer boundary (interface movement prescribed by $y = T$)

We use the diffusion coefficients $\kappa_1 = 1, \kappa_2 = 0.1$ and choose Dirichlet boundary data u^d and a right-hand side f such that the exact solution is given by

$$u(x,t) = \begin{cases} \sin(\frac{\kappa_2}{\kappa_1}(x_2 - t)), & x \in \Omega_1(t), \\ \sin(x_2 - t), & x \in \Omega_2(t). \end{cases}$$

In an interval $I_m = [t_{m-1}, t_m]$, we use the transformations

$$T_m(x,t) = \begin{cases} \left(x_1, x_2 - \frac{1+x_2}{1+t_m}(t_m - t)\right), & x \in \Omega_1(t), \\ \left(x_1, x_2 - t_m + t\right)), & x \in \Omega_2(t), \end{cases}$$

that fulfill the conditions of Assumption 3.1. In Figure 8, we plot the error at the end time $T = 0.512$ for the modified cG(1) scheme presented in this paper and a modified dG(0) scheme that is defined analogously using a $dG(0)$ Galerkin ansatz in time. We decrease the spatial and temporal discretization parameter simultaneously using $k = h$. As expected, we observe second-order convergence for the modified cG(1) scheme and first-order convergence for the modified dG(0) scheme.

Next, we study the effect of numerical integration and inexact projection schemes. First, we use a linear interpolation as projection from $\hat{\Omega}_h^{m-1}$ to $\hat{\Omega}_h^m$ after every time step. The interpolation operator i_h^m is defined by the relation

$$i_h^m u_{kh}^{m-1,+}(\hat{x}_i) = \left(\hat{u}_{kh}^{m-1} \circ T_m^{-1}(t_{m-1})\right)(\hat{x}_i)$$

in each grid point $x_i \in \hat{\Omega}^m$. Secondly, we use a summed midpoint rule with 64 points per patch for the evaluation of integrals like (43) instead of the exact quadrature scheme presented in Section 4.2.

In Figure 9, we compare the errors for these two schemes to the exact integration scheme. For the linear interpolation, we observe only linear convergence. As one would expect the projection error dominates the total error. The midpoint rule behaves similarly to our quadrature formula for larger time-steps k. For smaller time-step size, however, we observe again a reduction in the order of convergence. For $k = h \approx 10^{-2}$ the convergence rate is close to linear convergence. Here, again, the quadrature error becomes the dominant part of the total error. Our integration scheme, on the other hand, does not affect the quadratic convergence behaviour of the time stepping method.

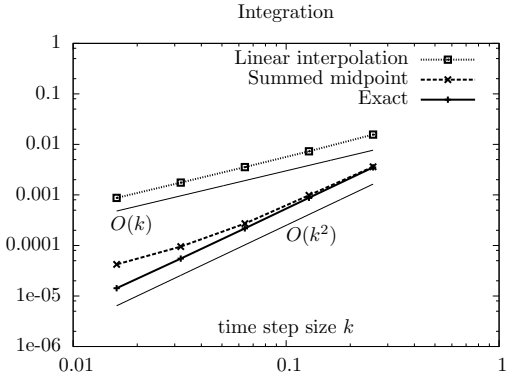

Figure 9. End time error for the modified cG(1) scheme applied to the model problem. We observe a reduced order of convergence when using non-exact integration formulas or projection schemes.

5.2 Rotating ellipsoid

As a second example, we consider a rotating ellipsoid $\Omega_{\text{ell}}(t)$ inside a fixed outer box $\Omega = [-1.2, 1.2]^2$ (see Figure 10). Initially, the ellipsoid has the Cartesian vectors as semi-principal axes with length 0.25 in vertical and 0.5 in horizontal direction. We apply a counter-clockwise rotation of the ellipsoid driven by the prescribed velocity field

$$\mathbf{v}^{\text{dom}} = 0.1 \begin{pmatrix} x_2 \\ -x_1 \end{pmatrix}.$$

Despite the fact that we could use this analytical velocity field to compute an analytical transformation T_m near the interface, we take a different approach here in order to show how to calculate a suitable transformation for realistic interface problems where the domain movement is only known at discrete points in time. A standard approach to capture the interface would be to define a scalar level-set function Φ that moves with the interface

$$\partial_t \Phi + \mathbf{v}^{\text{dom}} \cdot \nabla \Phi = 0 \quad \text{in } \Omega.$$

In order to define suitable transformations T_m, however, we follow a slightly different approach inspired by fluid-structure interaction problems [8]. We use the vector-valued Initial Point Set function $\Phi_{\text{IPS}}(t) : \Omega \to \mathbb{R}^2$ defined by the equation

$$\partial_t \Phi_{\text{IPS}} - \mathbf{v}^{\text{dom}} \cdot \nabla \Phi_{\text{IPS}} = 0 \quad \text{in } \Omega$$

with initial value $\Phi_{\text{IPS}}(t = 0) = \text{id}$. This function traces back points $x \in \Omega_{\text{ell}}(t)$ to their original position in $\Omega_{\text{ell}}(0)$. Thus, we can define the inner subdomain $\Omega_{\text{ell}}(t)$ by setting

$$\Omega_{\text{ell}}(t) = \{x \in \Omega,\ \Phi_{\text{IPS}}(x, t) \in \Omega_{\text{ell}}(0)\}$$

and the outer domain is given by $\Omega_2(t) = \Omega \setminus \overline{\Omega}_{\text{ell}}(t)$. Note that we do not define any spatial boundary conditions for Φ_{IPS}, as this could lead to a degeneration of the function before a full rotation of the ellipsoid is complete. Using the Initial Point Set function Φ_{IPS}, it is straight-forward to define a map that maps $\Omega_{\text{ell}}(t_m)$ to $\Omega_{\text{ell}}(t)$ and $\Gamma_i(t_m)$ to $\Gamma_i(t)$ such that for $t \in I_m$

$$\tilde{T}_m(t) = (\Phi_{\text{IPS}}(t))^{-1} \circ \Phi_{\text{IPS}}(t_m).$$

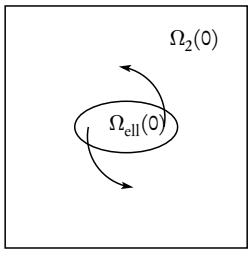

Figure 10. Subdomains of the second test configuration. The ellipsoid rotates counter-clockwise, while the outer domain Ω is fixed.

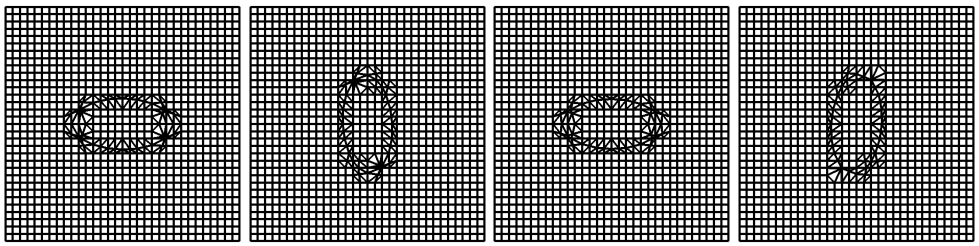

Figure 11. Spatial grid at time $t = 0, t = 15, t = 30$ and $t = 45$. The ellipsoid rotates counter-clockwise.

In our practical implementation, we determine the point $x^{m-1} := T_m(x^m) \in \Omega(t_{m-1})$ by solving

$$\Phi_{\text{IPS}}(t_{m-1})(x^{m-1}) = \Phi_{\text{IPS}}(t_m)(x^m)$$

with Newton's method and extend it linearly to the time interval I_m. To map the outer domain $\Omega_2(t_m)$ to $\Omega_2(t)$, we use an interpolation between the movement at the interface and the identity, id, at the outer boundary $\partial\Omega$

$$T_m(t) = g(x)\tilde{T}_m(t) + (1 - g(x))\text{id}.$$

where g denotes a smooth function with $g = 1$ in $\Omega_{\text{ell}}(t_m) \cup \Gamma(t_m)$ and $g = 0$ on $\partial\Omega$.

As data, we choose $f = \sqrt{(1 + \cos(5t))}$ as well as homogeneous initial data $u^0 = 0$ and Dirichlet data $u^d = 0$. The diffusion coefficients are again given by $\kappa_1 = 1$ and $\kappa_2 = 0.1$. The movement of the ellipsoid as well as the spatial grid are illustrated in Figure 11.

To study convergence, we compare the functional values for $||u_k(T)||_{\Omega(T)}$ and $||u_k||_Q$ for different time step sizes k, grid size $h = k$ and a modified cG(1) as well as a modified dG(0) scheme in Table 1. Furthermore, we calculate an extrapolated value e_0 as well as an estimated convergence order α by a least squares fit of the function $e(k) = e_0 + ck^\alpha$. For both functionals, we observe second-order convergence for the modified $cG(1)$ approach and first-order convergence for the $dG(0)$ variant. Finally, we plot the errors over the mesh/time-step size $h = k$ in Figure 12 to illustrate the convergence behaviour.

6 Conclusion

We have presented a time-stepping scheme for parabolic interface problems with a moving interface. The method is based on a Galerkin formulation of Crank-Nicolson type. To obtain the optimal order of convergence we use space-time test- and trial-functions, that are aligned with the moving interface. The resulting method is in each time step equivalent to a standard Galerkin approach

	$\|\|u_k(T)\|\|_\Omega$		$\|\|u_k\|\|_Q$	
$k = h$	dG(0)	cG(1)	dG(0)	cG(1)
0.15	0.619	0.5858	2.121	2.1286
0.075	0.605	0.5890	2.134	2.1423
0.0375	0.598	0.5899	2.140	2.1456
0.01875	0.594	0.5900	2.143	2.1463
Extrap.	0.589	0.5901	2.146	2.1466
Conv.	0.87	2.01	1.11	2.08

Table 1. Functional values for the ellipsoid problem in the space-time L^2-norm and in the L^2-norm at time $T = 15$ for a modified $dG(0)$ and a modified $cG(1)$ time stepping scheme and $k = h$. Furthermore, we give an extrapolated functional values for $k = h \to 0$ and estimate the convergence orders. The convergence orders are in good agreement with the theoretical predictions.

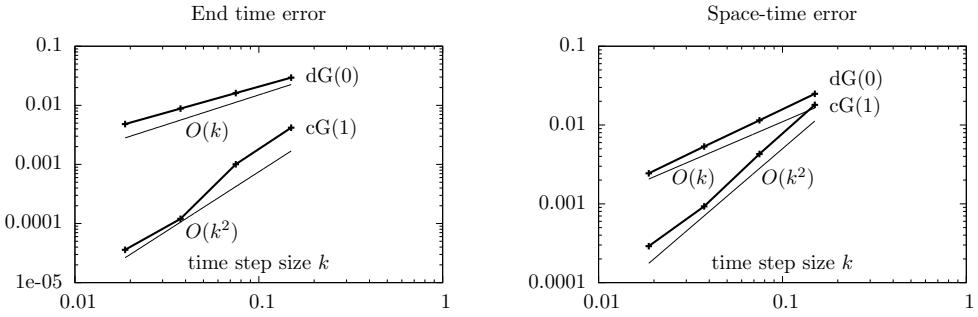

Figure 12. Functional errors for the ellipsoid problem in the end time L^2-norm and the L^2-norm over the space-time domain Q for $h = k \to 0$. As our theoretical results predict, we observe second-order convergence for the modified $cG(1)$ approach and first-order convergence for a modified $dG(0)$ approach.

applied to an ALE formulation on a fixed reference domain. For realization, the Galerkin formulation is approximated by suitable quadrature rules on every space-time slab. For this numerical approximation, we prove second order convergence in the L^2-norm in time and for the error at the end time. While we require the typical regularity of the unknown solution, a very smooth interface motion is needed. Numerical tests demonstrate the expected order of convergence.

Problems with moving interfaces appear in various application fields, such as multiphase flows or fluid-structure interactions. Future work will focus on the efficient application of the time-stepping scheme to such complex applications.

References

[1] A. Aziz and P. Monk. Continuous finite elements in space and time for the heat equation. *Math. Comp.*, 52:255–274, 1989.

[2] I. Babuška. The finite element method for elliptic equations with discontinuous coefficients. *Computing*, 5:207–213, 1970.

[3] Eberhard Bänsch and Stephan Weller. Fully implicit time discretization for a free surface flow problem. *PAMM*, 11(1):619–620, 2011.

[4] Peter Bastian and Christian Engwer. An unfitted finite element method using discontinuous Galerkin. *International Journal for Numerical Methods in Engineering*, 79(12):1557–1576, 2009.

[5] J.H. Bramble and J.T. King. A finite element method for interface problems in domains with smooth boundaries and interfaces. *Advances in Computational Mathematics*, 6:109–138, 1996.

[6] Ramon Codina, Guillaume Houzeaux, Herbert Coppola-Owen, and Joan Baiges. The fixed-mesh ale approach for the numerical approximation of flows in moving domains. *J. Comp.Phys.*, 228(5):1591–1611, 2009.

[7] Georges-Henri Cottet, Emmanuel Maitre, and Thomas Milcent. An eulerian method for fluid-structure coupling with biophysical applications. In *ECCOMAS CFD 2006: Proceedings of the European Conference on Computational Fluid Dynamics, Egmond aan Zee, The Netherlands, September 5-8, 2006*, 2006.

[8] Thomas Dunne and Rolf Rannacher. Adaptive finite element approximation of fluid-structure interaction based on an eulerian variational formulation. In *Fluid-structure interaction*, pages 110–145. Springer, 2006.

[9] R. Dziri and J.-P. Zolésio. Eulerian derivative for non-cylindrical functionals. In *Shape optimization and optimal design*, volume 216, pages 87–108. J. Cagnol, M.P. Polis, J.-P. Zolésio, 2001.

[10] K. Eriksson, D. Estep, P. Hansbo, and C. Johnson. *Computational differential equations*. Cambridge Univ. Press, 1996.

[11] Stefan Frei. *Eulerian finite element methods for interface problems and fluid-structure interactions*. PhD thesis, Universität Heidelberg, 2016 (to appear).

[12] Stefan Frei and Thomas Richter. A locally modified parametric finite element method for interface problems. *SIAM Journal on Numerical Analysis*, 52(5):2315–2334, 2014.

[13] Thomas-Peter Fries and Andreas Zilian. On time integration in the xfem. *International Journal for Numerical Methods in Engineering*, 79(1):69–93, 2009.

[14] J. Heywood and R. Rannacher. Finite-element approximation of the nonstationary navier–stokes problem. part iv: Error analysis for second-order time discretization. *SIAM J. Numer. Anal.*, 27(2):353–384, 1990.

[15] Christoph Lehrenfeld and Arnold Reusken. Analysis of a nitsche xfem-dg discretization for a class of two-phase mass transport problems. *SIAM Journal on Numerical Analysis*, 51(2): 958–983, 2013.

[16] N. Moës, J. Dolbow, and T. Belytschko. A finite element method for crack growth without remeshing. *Int. J. Numer. Meth. Engrg.*, 46:131–150, 1999.

[17] T. Richter. *Finite Elements for Fluid-Structure Interactions*. Springer, 2016. in preparation.

[18] Yogaraj Sudhakar and Wolfgang A Wall. Quadrature schemes for arbitrary convex/concave volumes and integration of weak form in enriched partition of unity methods. *Computer Methods in Applied Mechanics and Engineering*, 258:39–54, 2013.

[19] Paolo Zunino. Analysis of backward euler/extended finite element discretization of parabolic problems with moving interfaces. *Computer Methods in Applied Mechanics and Engineering*, 258:152–165, 2013.